Development Progress of Coating First Wall Components with Functionally Graded W/EUROFER Layers on Laboratory Scale

Thomas Emmerich^{a,1}, Dandan Qu^a, Jörg Rey^b, Bradut-Eugen Ghidersa^b, Robert Vaßen^c, Jarir
Aktaa^a

^aKarlsruhe Institute of Technology (KIT), Institute for Applied Materials, Hermann-von-Helmholtz-Platz 1, 76344 Eggenstein-Leopoldshafen, Germany

^bKarlsruhe Institute of Technology (KIT), Institute of Neutron Physics and Reactor Technology, Hermann-von-Helmholtz-Platz 1, 76344 Eggenstein-Leopoldshafen, Germany

^cForschungszentrum Jülich GmbH (FZJ), Institute of Energy and Climate Research, Wilhelm-Johnen-Straße, 52425 Jülich, Germany

For the First Wall of future fusion reactors, made of reduced activation ferritic martensitic steel, it is planned to use tungsten as protective coating, due to its favorable thermo-mechanical properties and low sputtering yield. The large difference in the coefficient of thermal expansion between steel and tungsten can be compensated by recently developed functionally graded material layers, inserted between the coating and substrate.

This paper gives first an overview of functionally graded W/EUROFER-layer systems, successfully produced on laboratory scale by vacuum plasma spraying and their achieved properties. Secondly, the current development status of transferring the coating process towards full scale First Wall components in form of Mock-ups is presented. For such components special attention needs to be paid to the challenges of a limited temperature window during coating, to achieve good coating adhesion, whilst avoiding exceeding the tempering temperature of the steel.

_

 $^{^{1}\} Corresponding\ author\ E-mail:thomas.emmerich@kit.edu$

Finally, the results of thermal tests of coated First Wall Mock-ups in HELOKA (HElium LOop KArlsruhe) under fusion relevant conditions and of the coating process development towards larger coating areas are reported.

Keywords: tungsten, first wall, functionally graded material (FGM), vacuum plasma spraying, finite element simulation.

1. Introduction

For First-Wall (FW) components of future fusion power plants it is envisaged to protect the steel structures against the plasma using tungsten (W)-coatings, because of its favorable thermo-mechanical properties and low sputtering yield. Functionally graded (FG)-layers between the W-coating and the steel substrate, e.g. the reduced activation ferritic martensitic steel EUROFER, compensate the difference in the coefficient of thermal expansion (CTE) [1]. In collaboration with the IEK-1 of Forschungszentrum Jülich [2] several batches of such layer systems were successfully produced [3–5] on laboratory scale using the vacuum plasma spraying (VPS) technique. The layer systems were tested in regard to their mechanical and thermal properties and encouraging results were gained. The measured layer properties are presented in this paper, together with the experimentally determined and utilized spraying parameters. Due to the positive results on material samples and in view of future, large scale FW components, two respective FW Mock-ups were produced and coated. After verifying that the coating was successful, one of these Mock-up was prepared and the coatings durability positively tested under fusion relevant heat loads and Helium (He)-coolant flows. Furthermore, another, larger Mock-up was produced in parallel, because of the achieved coating on the smaller Mock-up, and also successfully coated after an optimization of the coating, supported by finite element (FE)-simulations.

2. Production of functionally graded W/EUROFER coatings

2.1. Spraying parameters

In this section an overview of the powder and spraying parameters used for producing the layer systems on laboratory scale is given. In regard to the coating materials, stock W-powder "AW3105" from the company "Eurotungstene" is used with, according to its datasheet, a guaranteed W-content of at least 99.86 mass-% and a mean particle size of about 12 μ m. EUROFER-powder was procured from the company "Nanoval", produced by mixing the parent materials in a melt, aiming for the target composition of EUROFER [6], and sprayed in Argon (Ar) in a way to achieve the chosen maximum particle diameter (D96 = 52 μ m) and thus a mean particle diameter of about 23 μ m (Figure 1).

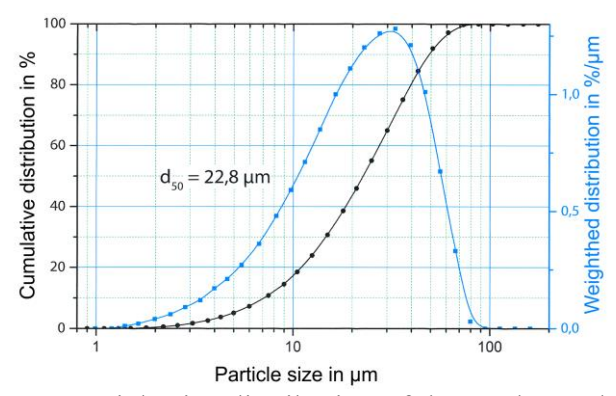


Figure 1. Particle size distribution of the steel-powder.

Specifically for the coating of Mock-ups, the composition of the received powder was controlled by chemical analysis of which the average values are listed in Table 1. Compared to the target composition of EUROFER [6] the tantalum (Ta)- and the nitrogen (N)-content are lower, whereas the oxygen (O)-content is higher than specified. The standard deviation amounts for the parent element iron (Fe) to 0.1 mass-% and for the alloying elements generally to less than 0.02 mass-%.

Table 1. Average steel-powder composition in mass-%.

С	N	O	V	Cr	Mn	Fe	Ta	W
0.090	0.004	0.056	0.199	8.730	0.396	Bal.	0.059	1.081

Coating on laboratory scale was performed at Forschungszentrum Jülich utilizing a plasma sprayer "F4" from the company "Oerlikon Metco". Table 2 lists the latest process parameters used for coating [2]. The metal powders are injected separately into the plasma by two internal injectors inside the equipped nozzle (Ø8 mm diameter). Both injectors are located at the bottom of the nozzle, with an angle of 45 ° between each other, to align the powders trajectories in the plasma plume and ensure homogenous material distribution on the substrate [2].

The feeding rates for EUROFER- and W-powder are in the range of 28 g/min and 55 g/min, respectively [2]. By varying the feeding rate of both powders, the functional gradation is created.

Table 2. VPS process parameters for W- and FG W/EUROFER-coatings [2].

	Current in A	Power in kW	Spraying distance in m	Argon volume stream	Hydrogen volume stream	Chamber pressure in mbar	Spraying system relative speed in m/s
				in slpm	in slpm		
Standard							0.44
Faster speed	680–750	50–51	0.3	40	11.5	60	0.5

The greatest challenge during coating EUROFER is the temperature window: On the one hand the substrate temperature should not be too low to ensure adhesion of the coating, on the other hand the temperature should not exceed the substrate tempering temperature as otherwise the material strength decreases. To cope with the latter, the plasma plume is regularly moved from the sample to let the substrate cool down before it reaches its tempering temperature. Furthermore, coating can also be conducted with a faster spraying system movement speed of 0.5 m/s, which moderates the hardness loss of the material [4] without affecting the layer adhesion significantly [7]. The faster movement shortens the local contact time between plasma plume and substrate and reduces thus the amount of heat the sample surface receives, so that the substrate stays below its tempering temperature. The coating process control can be further improved, when a suitable online monitoring of the substrates internal temperature is available.

2.2. Achieved layer properties

The first FG W/EUROFER VPS-coatings were created in a previous project for divertor application [8,9] and deposited on Ø10 mm cylindrical samples of a W/W-alloy substrate with a thickness of up to 1 mm and three gradation steps. These layer systems were tested in regard to their high temperature stability and it was shown that for the test time of 60 min the upper temperature limit can be extended up to 800 °C, because precipitation of Fe₂W intermetallic compounds (IMC) starts at about 900 °C [9].

In view of FW protection, coatings with a three- and five-step FG-layers as well as a W-top coat were successfully deposited on $100\times100~\text{mm}^2$ large EUROFER substrates [3,5]. The total FG-layer thickness was in the range of 300 μ m to 700 μ m, while the W-top coat had a nominal thickness of 500 μ m [3,5]. The actual total thickness was generally thicker than the specified one, with deviations in the range of 50 to 200 μ m [3,5]. The interfaces between coating and substrate as well as between the FG-layer themselves were sound, without cracks or delaminations. The observed porosity of the W-top coat was generally \leq 5 % [3,5]. Of these layer systems $50\times10~\text{mm}^2$ large pieces were tested in regard to Edge-Localized-Modes (ELM)-like thermal shock loads, using the electron beam facility JUDITH 1 from FZJ. The samples withstood at least 100 single pulses at 0.19 GW/m² with a duration of 1 ms and 2 s pause in-between, to allow the samples to cool down completely [3,4]. Furthermore, the layer systems showed in form of cylindrical samples of 0.000 05×20 mm also no damage after 500 cycles of thermal fatigue between 350 and 550 °C in a vacuum furnace [3,4]. Finally, at 550 °C satisfactory layer adhesion was determined by fracture mechanical bending tests, while the fracture surfaces showed indications of metallurgical bonding [3].

Thicker layer systems with 1.2 mm thick FG-layers and 0.8 mm thick W-top coats were also successfully created on 50×50 mm² large EUROFER substrates [3,4] and thus the desired thickness of 2 mm for W-coatings achieved. A FG-layer thickness of 1.2 mm or higher is preferred, because

FE-simulations indicate that then the maximum creep strain per thermal cycle in the EUROFER substrate decreases significantly [1]. Fracture mechanical bending tests on these layer systems showed interface toughness values similar to the former layer systems and also indications of metallurgical bonding [7]. These layer systems were also tested in regard to thermal fatigue, between 300 and 550 °C for up to 5000 cycles, and exhibited neither deterioration of the coating itself nor of the coating/substrate interface [10].

During the process development of coating FW Mock-ups, with internal cooling channels and coating areas of 270×65 mm² and larger, unsuccessful coatings detached as shown later. From these coatings Ø12 mm disks were cut from random locations by electrical discharge machining (EDM) and the thermal diffusivity measured by laser flash. The specific values of the four samples tested, each two for the pure W-top coat and for the complete 2 mm thick layer system, are plotted in Figure 2 a. The several data points have a good congruency to each other, as their deviation to each other is less than the 5 %, which is indicated by the error bars. In comparison to the literature data of W [11], the average measured W-values are closer to bulk- than to VPS-W (Figure 2 b), which corroborates the use of the former data in previous works [7]. The higher agreement with the bulk-W values could be due to the low porosity achieved during production. In comparison to EUROFER [12] (Figure 2 c) the coating exhibits a slightly higher thermal diffusivity, likely because its last layer is not pure EUROFER, but consists out of 75 Vol.-% EUROFER and 25 Vol-% W. This indicates also that the thermal diffusivity through the coating is limited by the least conductive component.

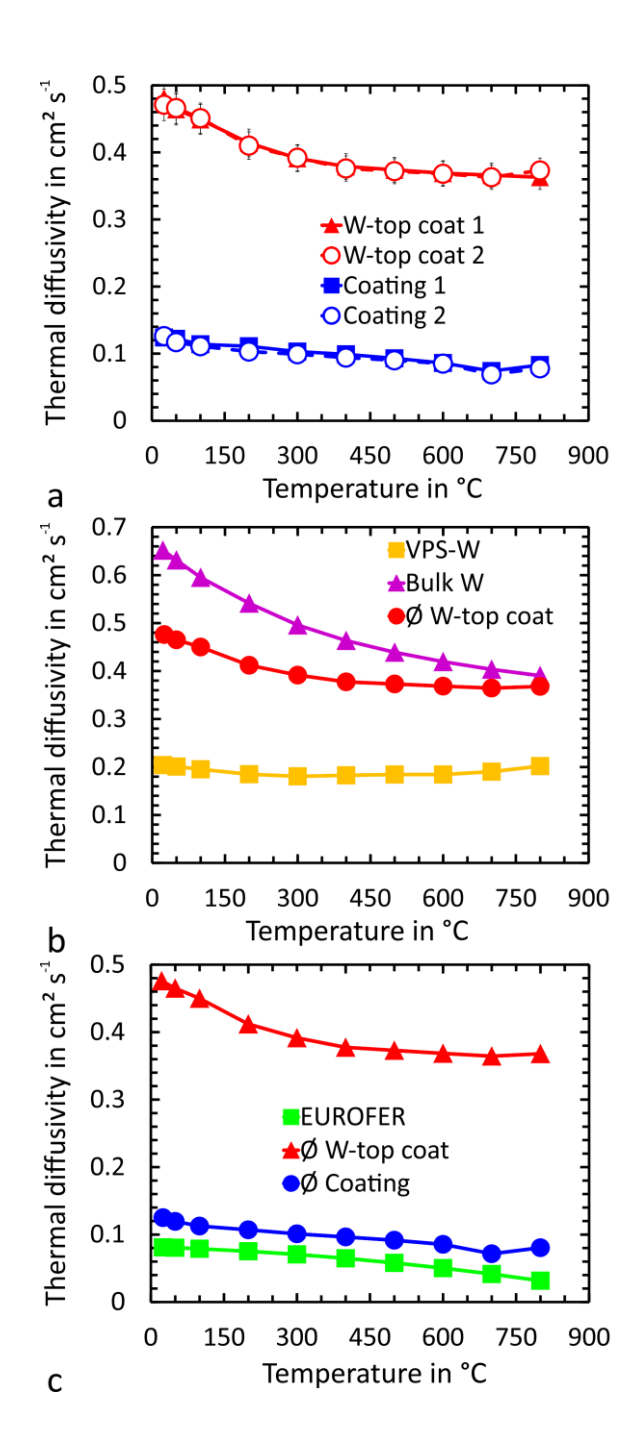


Figure 2. Measured thermal diffusivity and comparison of (a) the individual samples to each other, (b) to mean measured value of the W-top coat to literature data of W [11] and (c) the measured values to literature data of EUROFER [12].

3. Production and testing of First-Wall Mock-ups

3.1. Production of First-Wall Mock-ups

Due to the encouraging layer properties and in view of real size FW-structural components it was of interest whether coatings of similar quality and properties can also be deposited on structures with larger surface areas as well as with internal structures and how such layer systems behave under conditions comparable to future fusion reactors.

Two Mock-ups were fabricated out of 300×100×20 mm³ large EUROFER plates with three cooling channels, which have rectangular cross-sections of 10×15 mm², rounded corners (Figure 3) and were cut into the plates by EDM. The wall thickness between the channels and the plate's top surface are 5 and 4 mm, respectively. Into one of the channel walls a Ø1.5–18 mm hole was drilled from below for inserting thermocouples. To both ends of the plate first, simple manifolds made of EUROFER were welded by the tungsten inert gas (TIG)-technique. After welding, the Mock-ups were heat treated with austenitization at 1050 °C for about 90 min, cooling to 170 °C and annealing at 760 °C for about 90 min. The welding and heat treatment parameters were selected on basis of the guidance of the ferritic martensitic (FM)-steel 1.4901 (P92) [13]. For fixing the Mock-up in the holding frame during VPS, bores were drilled into the plate sides. Three of these four fixing points allow free movement in length and width, to avoid constrain stresses during coating. The coating, consisting of a 1.2 mm thick FG-layer and a 0.8 mm thick W-top coat, was sprayed onto the central part of the plate above the cooling channels on an area of 270×65 mm². A cover plate protected the rest of the Mock-up, especially the welding seams and the holding frame, against the spraying.

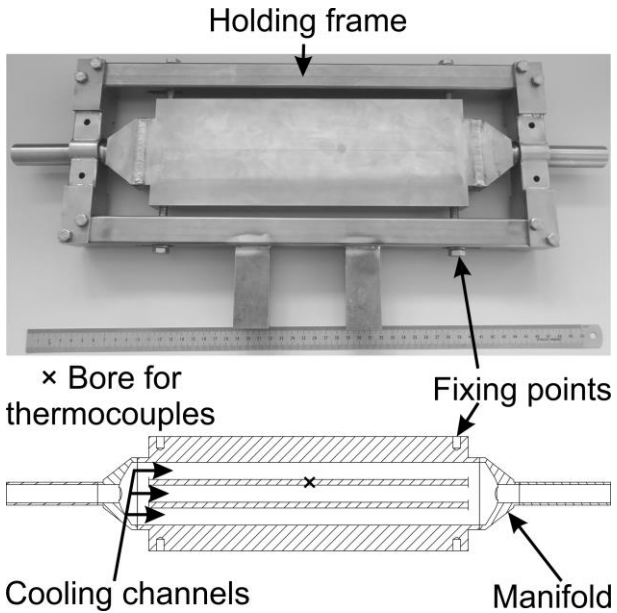


Figure 3. Mock-up after welding, fixed to its holding frame, and its schematic cross-section.

VPS was performed at Forschungszentrum Jülich and standard spraying parameters as well as spraying with faster robot speed were used (Table 2). The latter was specifically tested, because the cooling channels reduce the amount of material for heat transfer in the central area, so that local overheating and loss of material strength could be possible. Preheating of the plate was achieved by the plasma plume without powder injection. The surface and internal temperature of the Mock-ups during spraying were monitored using a pyrometer and by implemented Type-K thermocouples, respectively.

The temperature trends measured by the thermocouples during spraying with standard parameters are plotted in Figure 4 and for spraying with faster robot speed in Figure 5. During spraying with standard parameters (Figure 4) the maximum temperatures are near, but still below the materials annealing temperature of 760 °C. Cooling was achieved by removing regularly the plasma plume from the Mock-up. The significant temperature interruptions could be due to loose thermocouple connections. In regard to spraying with faster robot speed (Figure 5), more passes of the spraying system were needed to achieve the required layer thickness, which is reflected by the higher number of temperature changes than during spraying with standard parameters. Furthermore,

special attention was paid to achieve a lower maximum temperature than with standard spraying parameters, which was realized by removing the plasma plume more often from the Mock-up. Consequently, maximum temperatures of about 100 °C lower than for standard spraying parameters were accomplished. Hence, the faster spraying speed improves the coating in two ways: First, the local temperature increase is not as fast and secondly, due to the lesser amount of deposited material per pass, the coating could be produced more evenly.

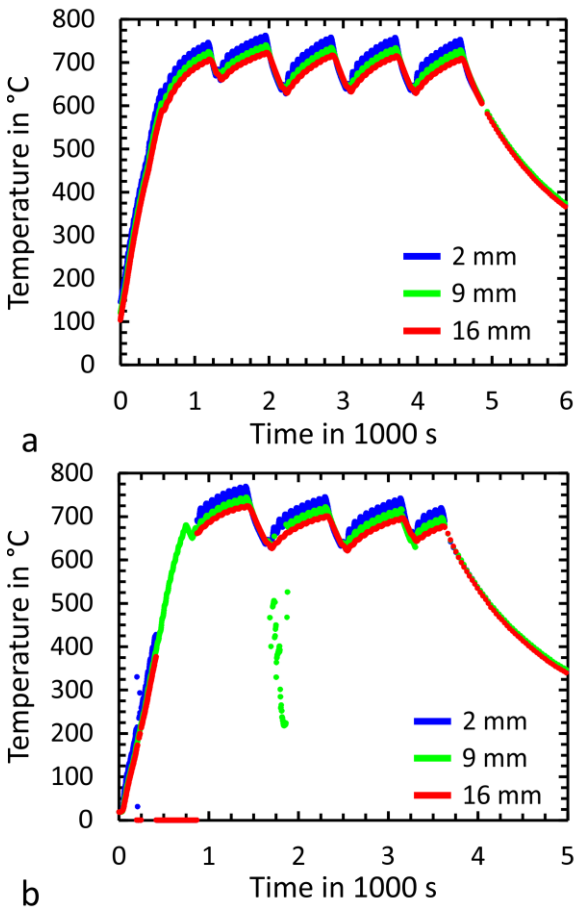


Figure 4.Temperatures in the first Mock-up, at different distances from the substrate top-surface, during coating (a) the FG-layer and (b) the W-top coat with standard spraying parameters.

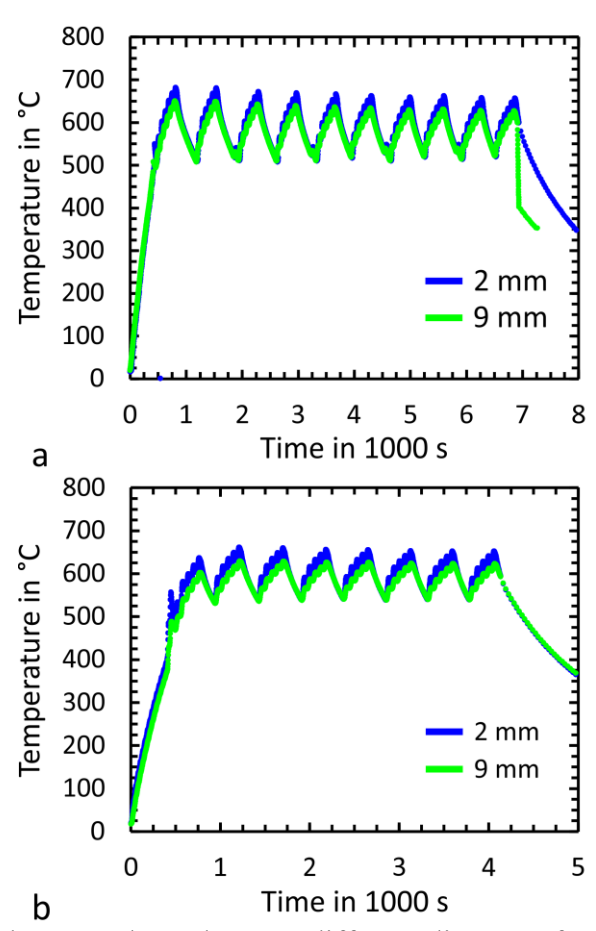


Figure 5. Temperatures in the second Mock-up, at different distances from the substrate top-surface, during coating (a) the FG-layer and (b) the W-top coat with faster spraying robot speed.

After coating no apparent external defects, e.g. delamination or cracks, were observed. To remove the unattached powder on the Mock-up, cleaning in an ultrasonic bath and dry ice blasting were tested, of which the latter produced better results and can also easily be used for larger components. A subsequent, corroborative defect control by dye penetration was also tried out, but produced no usable results, due to the coatings surface roughness and porosity.

The coatings were also controlled for internal defects by ultrasonic testing at a frequency of 10 MHz. For the coating an averaged sound velocity (5416 m/s) was estimated, based on the sound velocities of W (5200 m/s) and steel (5560 m/s), the corresponding FG-layer compositions and nominal thicknesses. Based on this averaged sound velocity and the measured signal travel time, the distance of the echo source is determined. This allows to analyze the produced information at a

specific depth, which is exemplary shown in Figure 6 for the Mock-up coated with standard spraying parameters. Depicted are the coating after dry ice blasting and the results of the ultrasonic testing for the calculated depth of 2 to 4 mm and 6 to 8 mm. These results represent the coating/substrate interface and the cooling channels, respectively. In regard to the interface, the results indicate that the signal amplitude is evenly reduced over the whole coating area, while in the latter all cooling channels are clearly depicted. Hence, no significant internal defects, like internal delamination, exist. In case of the Mock-up coated with faster robot speed, similar results are observed.

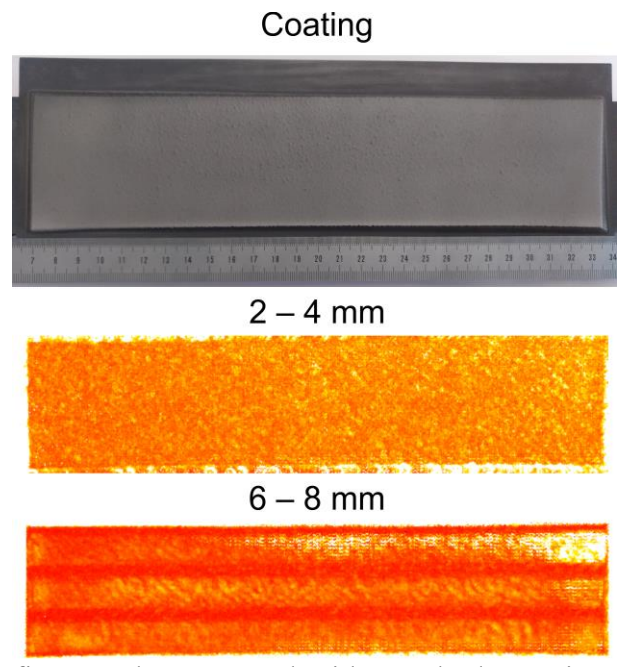


Figure 6. Top view on the first Mock-up, coated with standard spraying parameters, after dry ice blasting and the results from the ultrasonic testing below.

Due to the encouraging results it was decided to test one Mock-up under fusion relevant conditions. To ensure a homogeneous He distribution into all cooling channels, new manifolds were developed with an internal 90 °-turn. The manifolds were fabricated out of the FM-steel 1.4901, due to the availability of suitable thick plates, and attached to the plate of the Mock-up, coated with standard spraying parameters, by TIG-welding (Figure 7). Afterwards the Mock-up was subjected

to post welding heat treatment (PWHT) in a vacuum furnace for 2 h at 740 °C followed by furnace cooling. The heat treatment was conducted in a vacuum furnace to avoid oxidation of the W-coating, while the 740 °C are the lowest allowable annealing temperature, according to [13], to prevent certainly formation of Fe/W IMC [9]. After the PWHT the coating was still adherent and exhibited no defects. Radiographic inspection of the welding seams showed, however, that the seams were imperfect and required repair. Hence, the manifolds were cut from the plate, once more welded to it and the Mock-up subjected to the PWHT.

This latter procedure caused warping of the substrate plate in the range of about 1 mm transversal to the Mock-ups longitudinal axis and spall off of the W-top coat, whereas the FG-coating still adhered to the substrate and showed neither external nor internal, checked by ultrasonic testing, signs of delamination. Furthermore, the W-fracture exhibit surface plastic deformations and pull-offs of the powder splats at several locations (Figure 8), indicating that relevant adhesion existed between the FG-layer and the W-top-coat. Hence, the warping of substrate and perhaps also the many processing steps produced a residual stress and strain state in the whole Mock-up, which exceeded the layer adhesion strength and finally caused the W-top-coat to spall off. Parts of this spalled off W-coating were used for measuring the thermal diffusivity of the W-top coat. As the still adherent FG-coating showed no signs of delamination, the Mock-up was subjected to a pressure test, in regard to pressure vessel safety regulations (DIN EN 13445), and readied for testing in HELOKA.

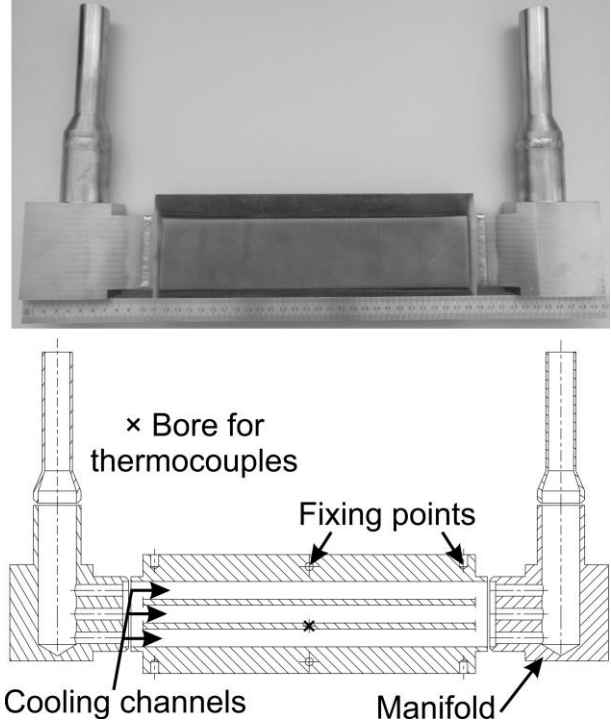


Figure 7. Top view and schematic cross-section of the Mock-up, coated with standard spraying parameters, after welding the new manifolds.

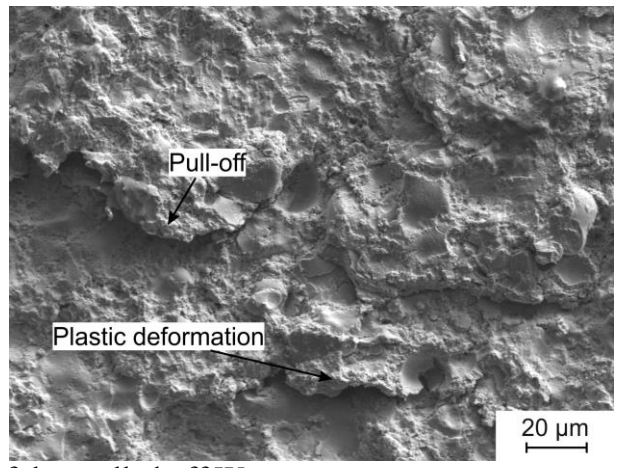


Figure 8. Fracture surface of the spalled off W-top coat.

3.2. Determination of testing parameters and thermal fatigue tests of FW Mock-up

The aim of testing the FW Mock-up in HELOKA was to confirm the durability of the coated Mock-up by exposing it under fusion relevant loadings as high as possible. The loading was applied as thermal cycles, leading to cyclic thermal stresses, which will cause higher strain on the coating system than holding at constant high temperature and thus closer to the coating systems stress free

state. The required test parameters were determined before, using a one dimensional calculation [14]. For the calculation, a single channel with the length L and the width w is considered. Furthermore, it is assumed that this channel receives only one uniform heat flux from one side with the density \dot{q} , while He flows with a mass flow rate of \dot{m} , an inlet temperature of T_1 , and a mean specific heat capacity \bar{c}_p through the channel. The resulting He outlet temperature T_2 can then be determined, by the equation [14]:

$$T_2 = T_1 + \frac{\dot{q}Lw}{\dot{m}\bar{c}_p}.\tag{1}$$

The calculated He outlet temperature can then be implemented into the equation

$$T_{\text{max}} = T_2 + \dot{q} \left(\frac{1}{h} + \frac{s}{\lambda} \right) \tag{2}$$

to identify the maximum surface temperature T_{max} of the FW, as it is of interest to not exceed the materials maximum working temperature. s represents the wall thickness between the heated and the cooled surfaces with the heat conductivity λ of the wall material and h the heat transfer coefficient from the solid wall into the He stream.

In regard to the produced Mock-ups, the dimensions L, w and s are 0.3, 1.5×10^{-3} and 4×10^{-3} m, respectively, while λ equals 25.94 W/m K. In case of He, a mass flow rate of 40 g/s and an inlet temperature of 300 °C are chosen. The mean specific heat capacity and the heat transfer coefficient are set to 5200 J/kg K and 7500 W/m² K, respectively. Finally, for the heat flux density a value in the range of $0.5 \le \dot{q} < 1$ MW/m² is expected [14]. For the mean value of \dot{q} , 0.75 MW/m², equations 1 and 2 produce under these assumptions a T_2 of about 316 °C and a $T_{\rm max}$ of about 532 °C. Furthermore, \dot{q} may even be increased to 0.80 MW/m², resulting in a maximum surface temperature of about 547 °C, without exceeding the maximum working temperature of EUROFER of 550 °C.

An overview of the selected testing criteria is given in Table 3. The maximum substrate temperature was decreased for the experiments to 520 °C, to further reduce the risk of a Mock-up

failure inside the test facility, in addition to the pressure vessel safety control, while the maximum coating temperature was limited to 800 °C to avoid formation of Fe/W IMC [9]. Finally, the Mock-up has to be pre-heated by He to 300 °C to avoid additional thermal stresses [7].

Table 3. Criteria for the heat flux tests in HELOKA.

Parameter	Value
Helium mass flow per channel	40 g/s
Pre-heating temperature	300 °C
Helium inlet temperature	300 °C
Helium pressure	8 MPa (abs.)
Maximum heat flux density	$\rightarrow 0.75 \text{ MW/m}^2$
Substrate temperature	≤520 °C
Surface temperature	≤800 °C
Number of cycles	1000

Based on these criteria the heat load and the He mass flow were step wised increased in preliminary tests, to achieve a heat flux density as high as possible, while the coating surface temperatures were monitored by a thermo-camera (Figure 9 a and c). In parallel the He temperatures and in particular the Mock-up internal temperature were determined (Figure 9 b). The latter was measured 2 mm below the substrate/coating interface by the implemented thermocouple in the center. The maximum temperature at that point was set to 500 °C, because of the thermal gradient that forms along the Mock-up, so that at the plate outlet side 520 °C are not exceeded. Concluding, due to the massive parts beside the cooling channels heating and cooling duration of 180 and 150 s were applied, respectively, to achieve steady-state over the whole plate. An overview of the final test parameters is given in Table 4.

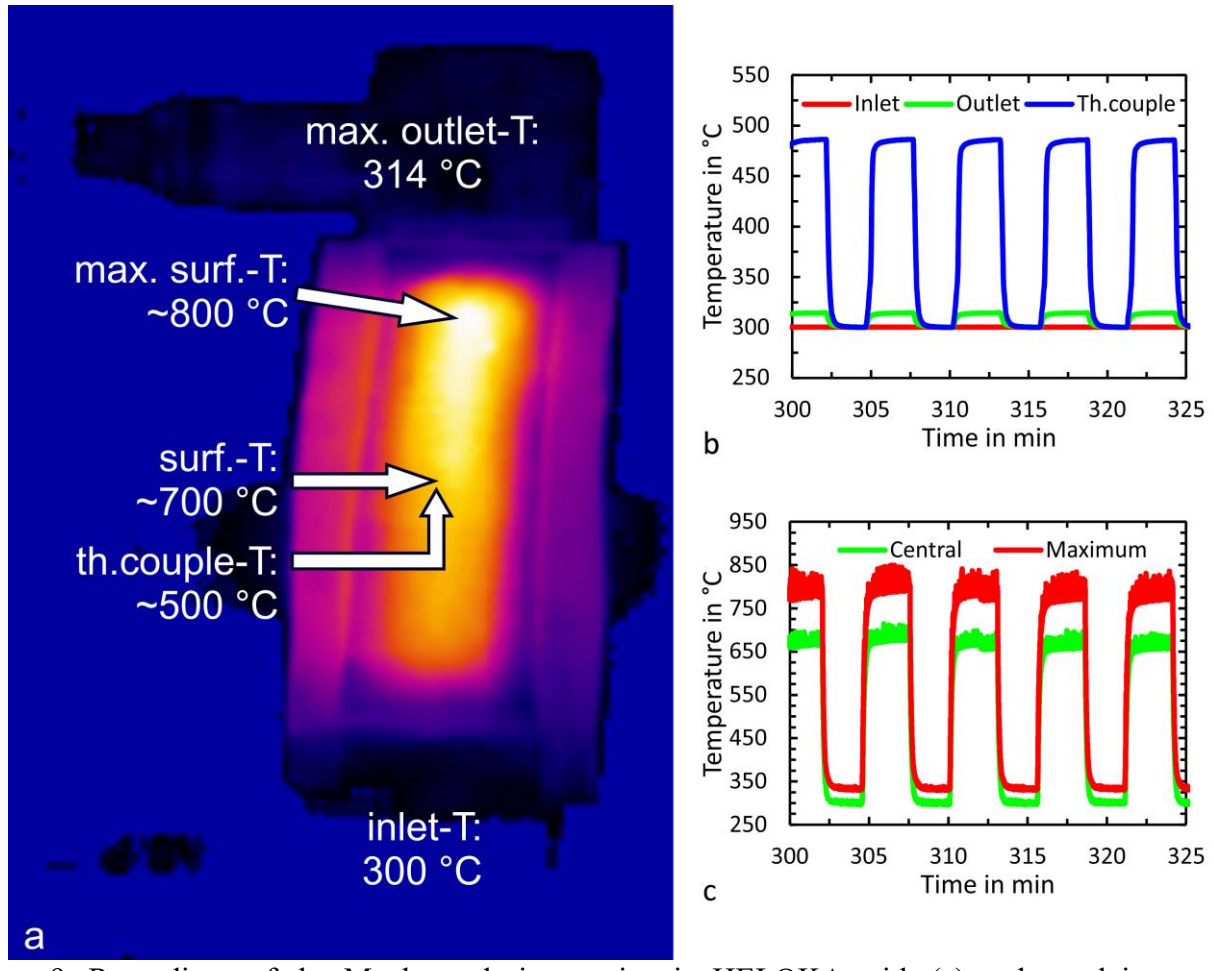


Figure 9. Recordings of the Mock-up during testing in HELOKA with (a) a thermal image at maximum heat load, (b) internal and (c) external temperatures.

Table 4. Testing parameters applied on the Mock-up in HELOKA.

Parameter	Value
Helium mass flow per channel	56.67 g/s
Pre-heating temperature	300 °C
Helium inlet temperature	300 °C
Helium pressure	8 MPa (abs.)
Maximum heat flux density	$0.7~\mathrm{MW/m^2}$
Heating and cooling time	180/150 s
Number of cycles	1000

3.3. Post exposure analysis

During thermal cycling no hotspots formed, what indicates that the coating did not detach during the heat flux tests. After the exposure material samples were cut out of the Mock-up by EDM. On these samples additional microstructural analyses were carried out to investigate, whether the substrate, the layer system changed or the coating interfaces may have deteriorated. Possible change of the substrate was evaluated in form of hardness profiles that were determined by using a Vicker indenter with a load of 9.81 N (HV1) and a minimum indent distance of 0.5 mm.

In this way, identical FW hardness profile trends (Figure 10) were determined at the inlet and outlet side of the Mock-up and a similar trend from the area below the maximum surface temperature during testing (Figure 9 a). Compared to the hardness profiles of the second Mock-up (Figure 11), which was specifically coated at about 100 °C lower maximum temperature, the substrate tempering temperature of the first Mock-ups was thus apparently slightly exceeded during the coating process, as hardness loss exists but is limited to a depth of about 4 mm. It follows also from these hardness profiles that the heat did not accumulate locally above the channels, possibly due to the lesser amount of material, what would have led to different temperatures and thus hardness losses.

In view of the quantitative hardness values at the three different locations, the sample from the high temperature area (Figure 10 c) exhibits, despite the scatter, a nearly 2 mm deeper and more distinct hardness loss, about 0.05 GPa, than the other two samples (Figure 10 a and b). As hardness loss caused also by temperatures above tempering temperature can be ruled out, it indicates that in this area the number of thermal cycles and particularly the temperatures were sufficient to allow significant thermo-cyclic softening.

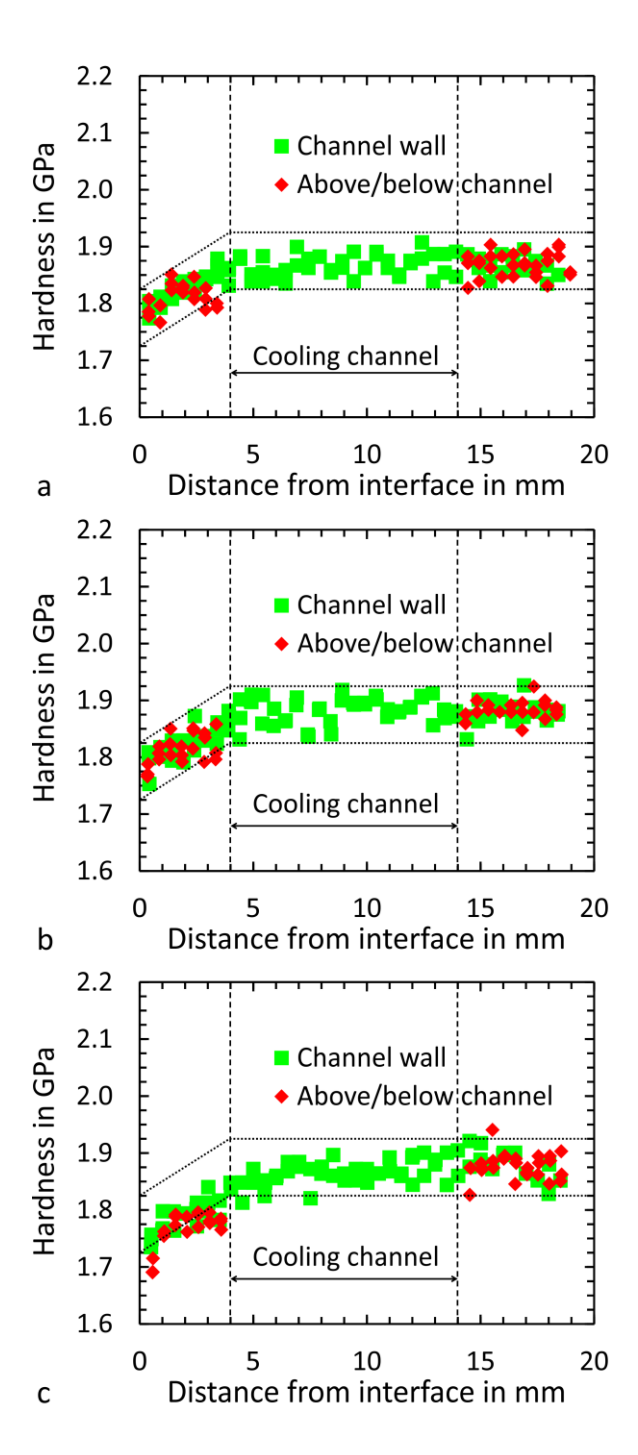


Figure 10. FW plate hardness profiles, with additional boundary lines as orientation guides, of the Mock-up tested in HELOKA at (a) the inlet, (b) outlet side and (c) from the high temperature area during exposure (Figure 9).

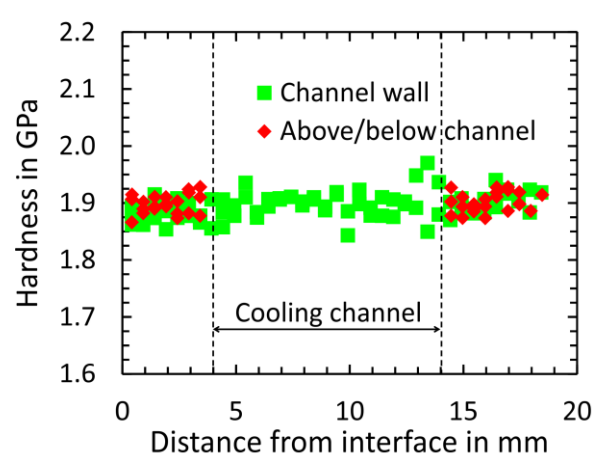


Figure 11. FW plate hardness profiles of the Mock-up coated at lower maximum temperature.

In regard to the coatings microstructure, the first aspect that catches the eye in the samples cross-sections (Figure 12) is that apparently not the entire W-top coat has spalled off but about 50 to 100 µm still adhere to the FG-layer. Additionally, the cross-sections reveal that the FG-layer is about 100 to 200 µm thicker than specified, while the coating microstructures are generally similar to each other. At all three locations the coatings exhibit no deterioration of the coating/substrate interface, in form of delamination or crack growth parallel to the coating/substrate interface. Hence, the thermal conductivity of the whole coating system did not diminish, what corroborates the observations made with the thermo-camera during testing.

On the other hand, Figure 12 c depicts areas with a comparable higher amount of pores or cavities that appear locally in that sample. As possible origin the production process can be ruled out first, because of the cavities irregular local appearance. Also growth or coarsening of pores seems unlikely, since the other two regions exhibit no significant amount of small pores. It could be, however, that some coating particles broke out of the cross-section during preparation, due to loss of adhesion between the particles, what left these cavities. As there are no apparent groves starting from the cavities, the particle broke likely during the earlier stage of the preparation out of the coating. The possibility of particle loss is further emphasized by the figures made at higher magnification (Figure 12 e and f) from the high temperature area, which show that the cavities have

comparable size and shape like the brighter appearing W-particles. The de-bonding of the particles could have been induced by the mismatch in CTE on the microscopic scale between the individual W/steel particles under the thermal cyclic loading. To what extend such de-bonding was also influenced by residual stresses cannot be determined, due to the welding and PWHT induced warping as well as spall off of the W-top coat.

Furthermore, at high magnification some particles and areas, having a grey scale between the ones of W- and steel-particles, can occasionally be found in all three cross-sections, as exemplary indicated by the arrows in Figure 12 d to f. Based on the results of EDX spot analyses these particles could be types of (Cr-)/Fe/W IMC [15]. Since these particles appear neither in the high temperature areas towards the coating surface but only in the FG-layer at or below the W/steel ratio of 50/50 nor equally at the interfaces of particles, they precipitated very likely not during testing. Hence, these particles originate from the production process and could be, due the large coated and analyzed area, a statistical appearance. Particularly the large coating area increases the possibility for IMC, due higher amount of sprayed powder and thus the chance for in-flight particle reactions. Reactions inside the deposited coating are for these Mock-ups, on the other hand, unlikely, as the substrate temperatures were monitored and stayed clearly below 800 °C during the coating process.

Therefore, these observations underline the thermal stability of the coating, especially as this area experienced thermal loads for a much longer time, at least 2000 min based on duration at maximum temperature (Figure 9 c) times number of cycles, than the material samples reported in [9] (60 min). Secondly, the investigations revealed no apparent detrimental effect of the IMC on the coating, which can be due to their low amount and small size.

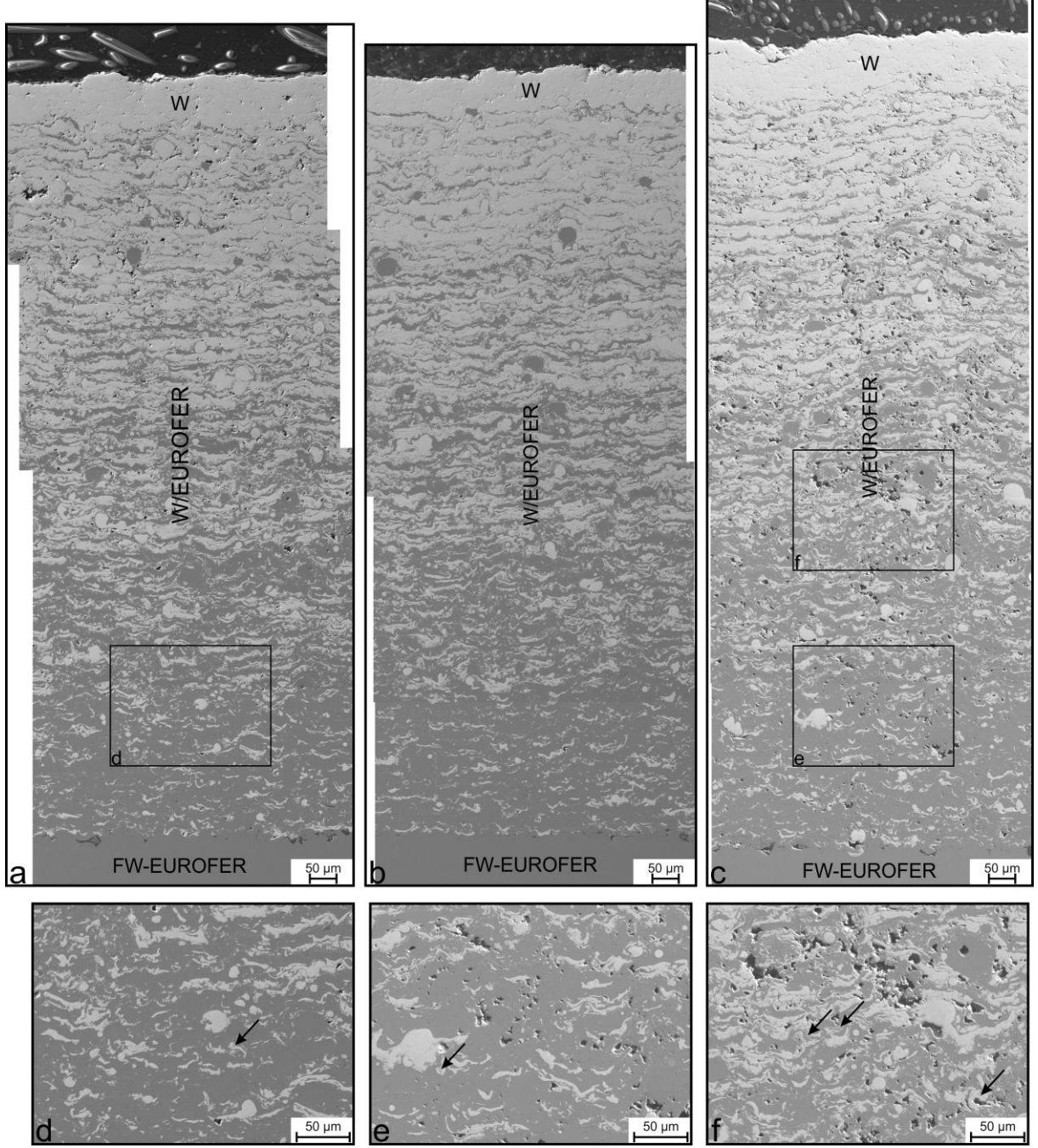


Figure 12. Cross-sections after thermal testing in HELOKA from (a) the inlet side, (b) the outlet side, (c) the high temperature area (Figure 9) of the Mock-up and (d–e) higher magnification of the marked areas.

Concluding, the test emphasizes the durability of the coating system under fusion relevant conditions. For future tests, it is of high interest to explore, how the layer system performs for

significant longer test duration or higher number of thermal cycles. During such tests the thermo-mechanical behavior, in particular thermo-cyclic softening or release of residual stresses, of the coating system with a complete 0.8 mm thick W-top coat and without additional influence from welding, needs to be investigated.

4. Production and coating larger FW Mock-ups

4.1. Coating using previous production process

Encouraged by to the successful coating of the Mock-ups another larger Mock-up was produced, parallel to the pressure vessel qualification and heat flux tests in HELOKA of the smaller Mock-up, in view of coating future full scale FW components. The Mock-up was manufactured out of an available 300×200×20 mm³ large EUROFER plate with five cooling channels that have rectangular cross-sections of 10×15 mm² with rounded corners (Figure 13), wall thicknesses to the top surface and in-between the channels of 4 mm and 5 mm, respectively, and special V-shaped ribs on the top side that increase the heat transfer between plate and cooling medium [16]. At seven different locations, lengthwise and crosswise to the longitudinal axis of the plate, Ø1.5-18 mm holes were drilled into the cooling channel walls for inserting thermocouples. Particular three positions, relative to the cooling channels longitudinal axis, were used for monitoring the temperatures during the coating process. For this Mock-up the further developed manifolds, made out of 1.4901 and with internal 90 °C-turns, were used and attached to the plate by TIG-welding. Afterwards, a complete hardening and tempering heat treatment was performed, similar to the previous kind of Mock-ups.

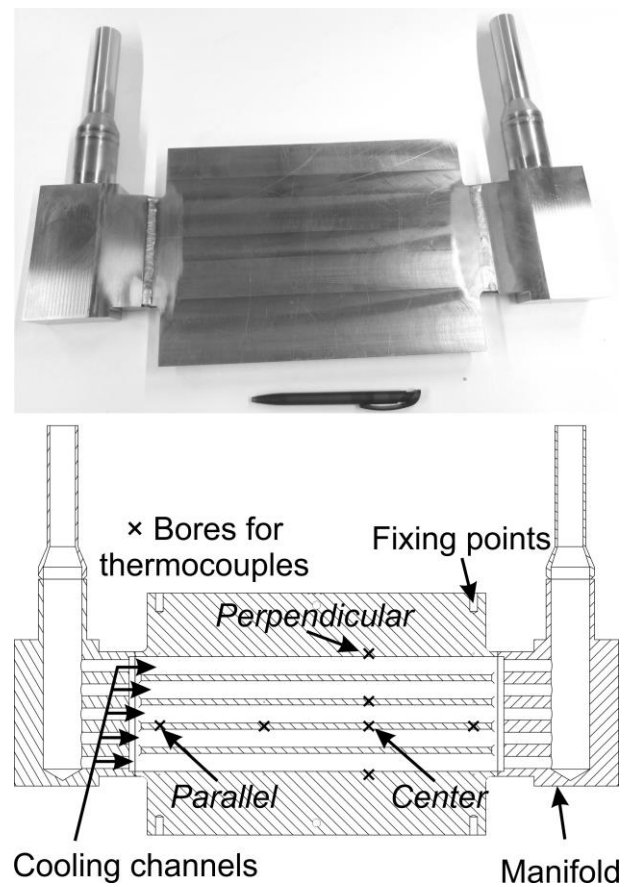


Figure 13. Second kind of Mock-up after fabrication and its schematic cross-section, with three particular thermocouple positions used for temperature monitoring.

For coating, the plate was preheated by the plasma plume without powder injection, while the coating itself was also applied to the central part above the cooling channels and covered an area of 270×115 mm². The coating was defined to consist out of a 1.2 mm thick FG-layer with a 0.8 mm thick W-top coat and was applied to the Mock-up at a spraying system speed of 0.5 m/s. A cover plate protected the holder, the side parts and especially the welding seams as well as the connecting tubes. Figure 14 depicts the internal temperature trends in the central area during deposition of the FG- and the W-layer. Like for the second test Mock-up, maximum temperatures of about 100 °C lower than the tempering temperature were achieved. The interruptions and restarts were due to problems with the facility: On the one hand as the heat management capacity of the facility was

reached, due to the large substrate and on the other hand as some layer material spalled off from the cover plate and blocked the manipulator mechanisms.

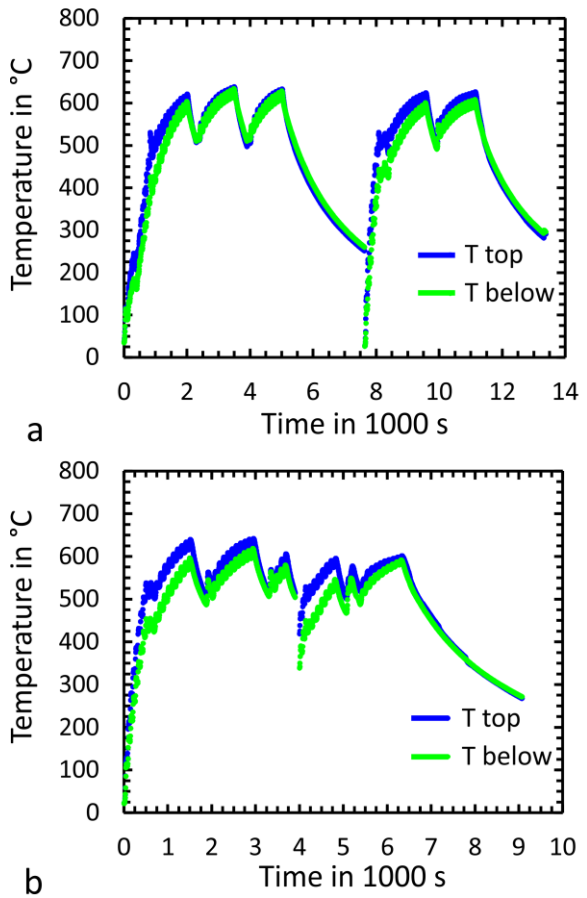


Figure 14. Temperatures in the larger Mock-up, at different distances from the substrate top-surface, during coating (a) the FG-layer and (b) the W-top coat.

After coating a crack and delamination at the coating corners were observed externally (Figure 15). In view of the ultrasonic analysis, the signal amplitude is significantly reduced near the externally visible delaminations. This implies that the delamination extends further beneath the surface, so that the coating adheres only to about one third of its area to the substrate.

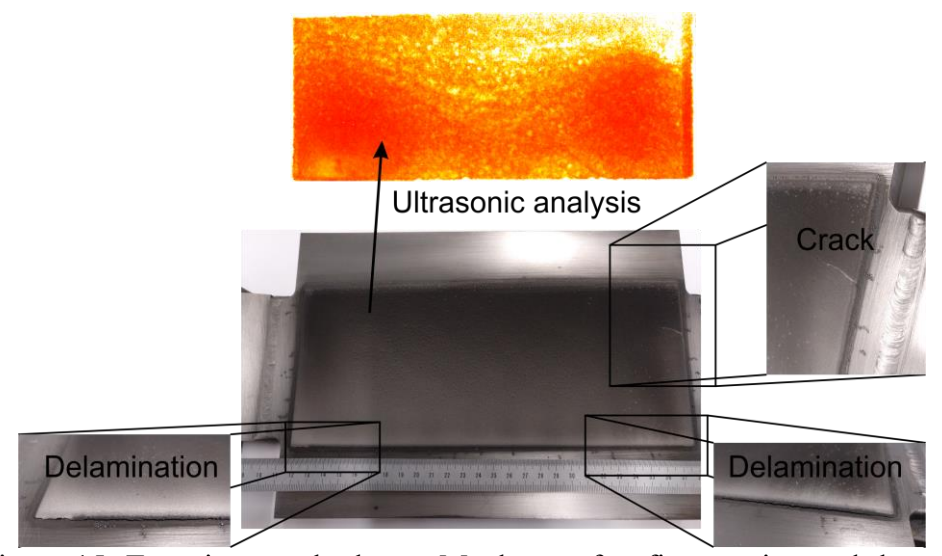


Figure 15. Top view on the larger Mock-up, after first coating and the results from the ultrasonic testing.

For anew deposition the layer system was removed and the substrate surface refurbished by mechanical means. Parts of the removed coating were used for measuring the thermal diffusivity of the whole layer system, shown above. In regard to its microstructure, the removed coating exhibits from an area with adhesion an uneven fracture surface (Figure 16) with plastic deformation, indicating that the structure adhered to the substrate and failed inside the coating itself during removal. In case of the coating from an area without adhesion, however, a comparatively even surface is visible, implying that the coating was already detached from the substrate before the removal. Hence, either the produced adhesion was too weak to compensate for the layer residual stresses or sufficient bonding between substrate and the first coating layer was not even produced.

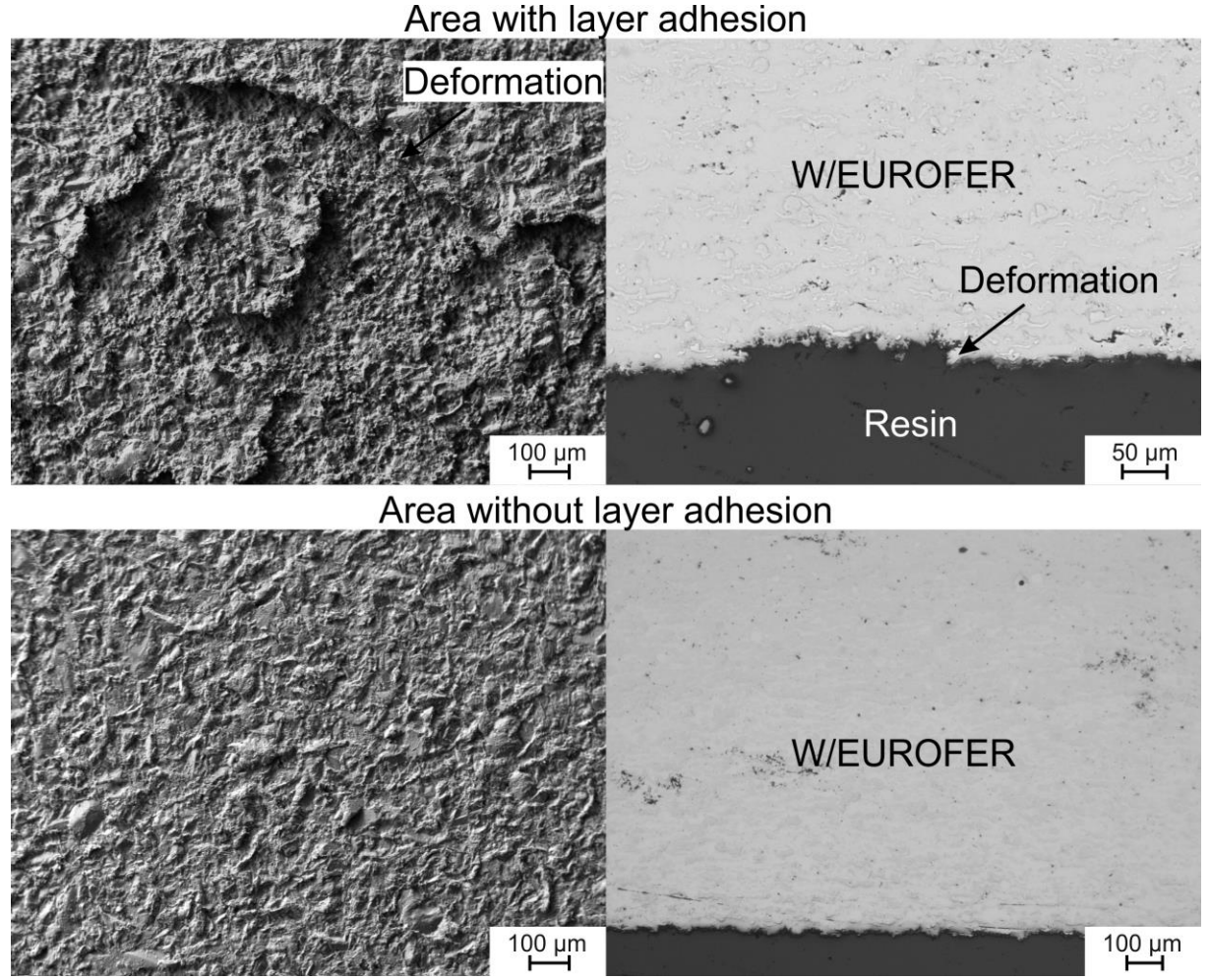


Figure 16. Surfaces and cross-sections of the removed coating at the coating/substrate interface from an area with and without layer adhesion.

To realise, notwithstanding, a successful coating two aspects were considered for modification: First, the layer cross-section could be modified to reduce the local maximum mechanical stresses; Secondly, the coating process could be adjusted to adapt to the larger component size, i.e. the preheating is adjusted to heat the higher thermal mass of the Mock-up to a required temperature level for formation of metallurgical bonding. The effects of these modifications were evaluated by FE-simulations, using the software ABAQUS [17], and in this way the parameters optimized for the anew coating.

4.2. FE-optimisation study for coating larger areas

4.2.1. Coating design

The modifications of the coating design were analysed on a cross-section of the Mock-up by thermomechanical simulations (Figure 17). The designs were evaluated in regard to minimise the von Mises stresses at the FG-layer edges.

For EUROFER and W the thermomechanical properties used are listed in Table 5. In regard to the FG-layer, the area was divided into five 240 µm thick sections and the material properties linearly interpolated to the corresponding W/EUROFER ratio. For W and the FG-layer linear-elastic and ideal-plastic material behaviour was assumed. In case of EUROFER, also linear-elastic behaviour was assumed and for plastic deformation additionally isotropic hardening, based on its ultimate tensile properties, was considered. The mesh consisted of "generalized plane strain"-elements with primarily quadratic form. Their maximum edge length was in the range between 0.06 and 1 mm, the smaller value especially used for the coating and the local area beneath the coating edges.

The simulation was conducted in form of a static analysis, by cooling down the homogeneous temperature field of the cross-section from its stress free state at 750 °C to 20 °C. The lower right corner of the EUROFER plate was fixed in x- and y-direction, while the lower left corner was restricted only in y-direction.

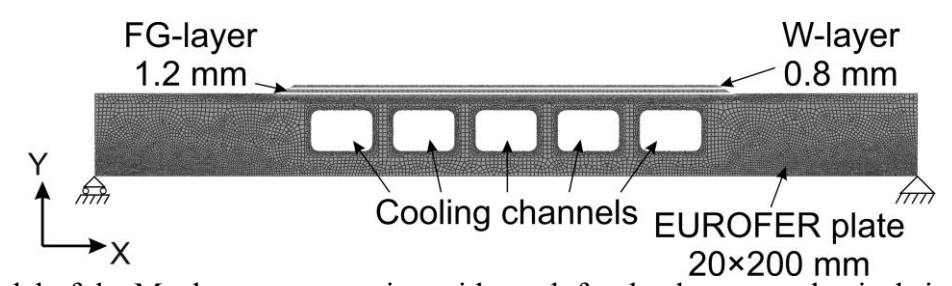


Figure 17. Model of the Mock-up cross-section with mesh for the thermomechanical simulations.

Table 5. Implemented elastic [8] and plastic [6] material properties for EUROFER and W.

			EUROFER				Tungste	en
Temperature in °C	Young's modulus in MPa		Ultimate tensile strength in MPa	Failure strain	Coefficient of thermal expansion in K ⁻¹	modulus	Yield strength in MPa	OVIDADION
20	217,260	545.57	794.61	0.1677		397,938	1360.46	
200	207,327	483.62	620.71			397,270	1154.17	
300				0.1309				
400	197,123	446.99	576.74	0.1362	1.20E-05	394,480	947.86	4.40E-06
500				0.1775	1.20L-03			4.40L-00
600	177,589	298.32	509.05	0.2659		389,508	764.79	
700	161,024	134.79	380.32	0.2963		386,210	681.67	
900	55,800	50	220.67			377,970	531.74	

In terms of the coating edge slopes, at a constant width of the uncoated area, an increase of the angle (e.g. 60 °) leads to a stress concentration at the corner of the coating (Figure 18). For smaller angles (e.g. 15 °), on the other hand, the stress fields are more evenly distributed, while beneath the edge the stress values are lower. Therefore, edges slopes lower than 30 ° are foreseen for anew coatings.

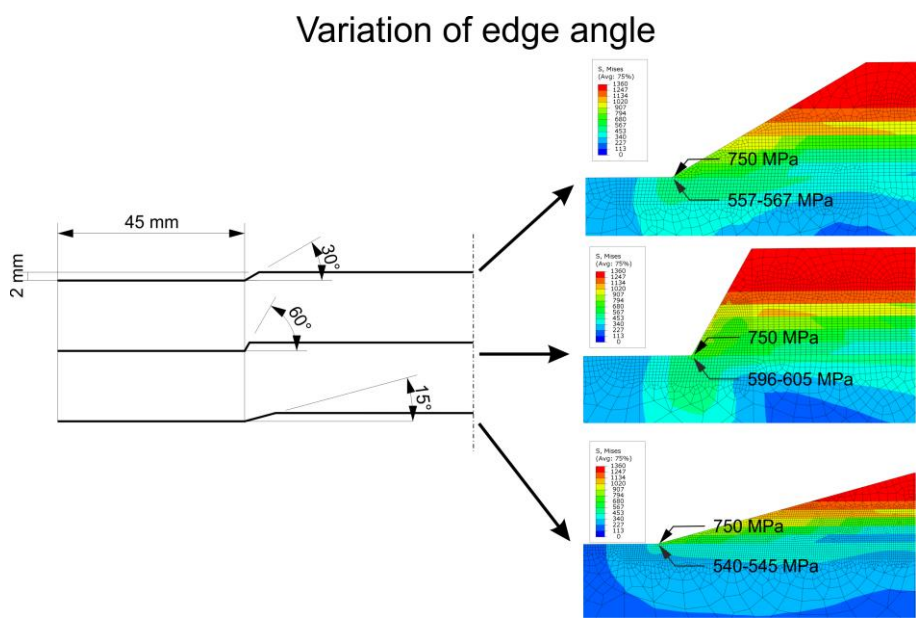


Figure 18. von Mises stresses at the coating edges as a function of the edge slope.

In view of the coating area (Figure 19), an increase onto 50 % of the previously uncoated side areas, the von Mises stress values beneath the edge stay similar to the previous simulation, whereas fields with von Mises stresses of about 340 to 570 MPa are broader. In case the coating is deposited to the whole width of the Mock-up, the stresses at the coating edge tip in the substrate and in the coating itself are significantly lower, which may be due to lower restrictions at the free edge. In regard to the fields of von Mises stresses in the range of 340 to 570 MPa, they cover an even larger area than in the previous case.

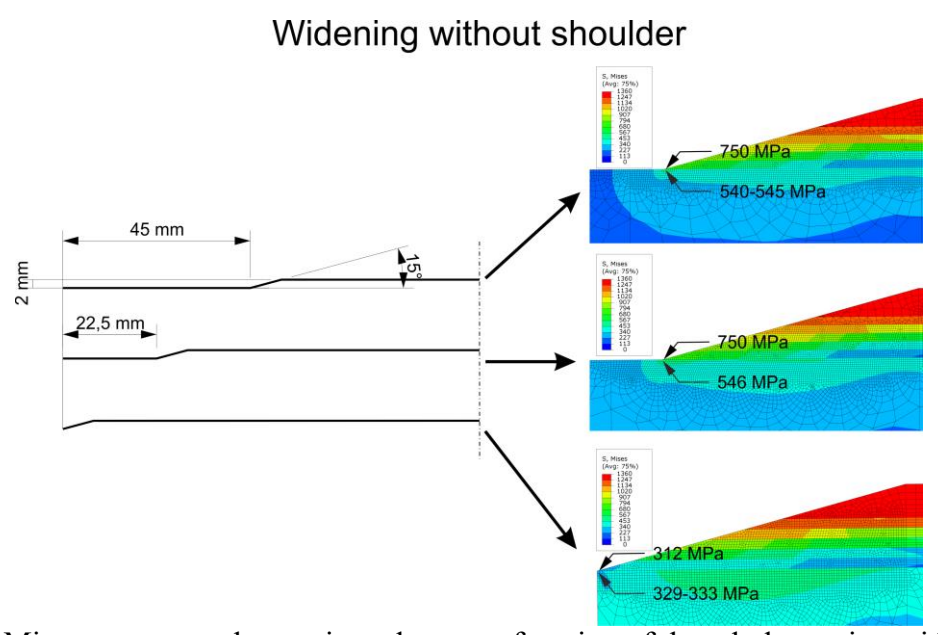


Figure 19. von Mises stresses at the coating edges as a function of the whole coating width.

Another option is to increase only the width of the FG-layer, whereas the W-layer remains the same (Figure 20) thus reducing the load on the FG-coating edge. This approach diminishes the fields with von Mises stresses of 340 to 570 MPa, compared to the previous simulations, and produces significantly lower stresses at the coating edge tip. Hence, the last design modification is chosen for anew coating.

Widening with shoulder

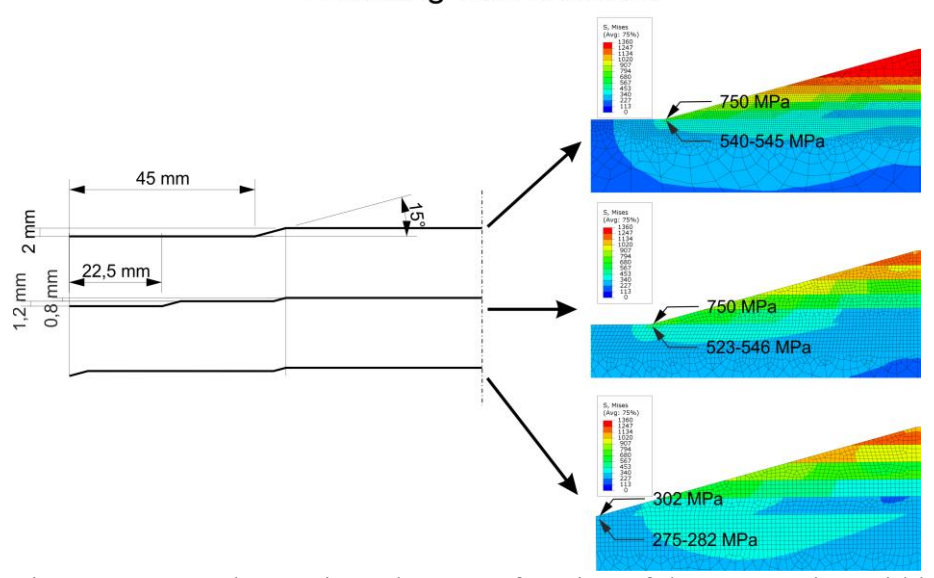


Figure 20. von Mises stresses at the coating edges as a function of the FG-coating width.

4.2.2. Coating process

In regard to the coating process, especially the preheating is of interest, to achieve on the whole coating area the required temperatures for the formation of metallurgical bonding, and was simulated by heat transfer simulations. The simulations were conducted on simplified models of the Mock-ups (Figure 21) to which the thermal properties of EUROFER (Table 6) are applied. For the three-dimensional geometries tetragonal heat transfer elements were used for convenience. Based on the temperature measurements depicted above, heat fluxes \dot{Q} from the spraying system were estimated and temperature distributions as well as trends simulated. For the fitting, the temperatures at the upper and lower node of a heat transfer element, which would be close to the thermocouples in the real Mock-ups, were compared to the measured ones.

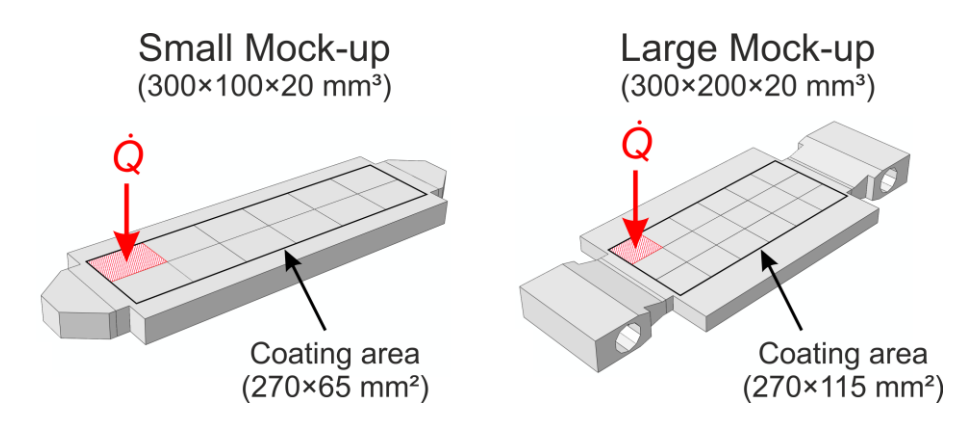


Figure 21. Models used for the simulations of the temperature distributions.

Table 6. Applied EUROFER properties for the heat transfer simulations [12].

Temperature	Thermal conductivity	Specific heat	Density
in °C	in W/mm K (Eq. 9)	in J/g K (Eq. 6)	in g/mm³
20	0.029333471	0.44810195	
200	0.031102651	0.51847092	
400	0.030119782	0.58454167	
600	0.031595950	0.79260167	0.00775
700	0.034995500	0.99990265	
800	0.042829894	1.30273094	
900	0.064402723	1.72109655	

The movement of the cone shaped spraying plasma was also taken into account in the simulation and set to 0.5 m/s. It was accomplished by first dividing the coating area equally into 45×32.5 mm² large fields, which shall represent the plasma cone area. Each of these fields was then heated by a heat flux that was linearly in- and decreased over time. Figure 22 gives a schematic visualization of the spot movement over the different field and the heat flux amplitudes as a function of time. The step duration equals 0.045 s and is calculated, for instance for the smaller Mock-up out of the necessary time of 1.08 s to cover the length of 12×45 mm at a speed of 0.5 m/s for an assumed number of 24 steps. A short cooling of the components between preheating and coating, due to the short removal of the plasma for introducing the powder, is also thinkable and was tested in form of a heat flow from the whole outer surface of the Mock-ups. This develops, however, significant discrepancies between the simulated and measured temperature trends, so that such cooling in-between was not further considered.

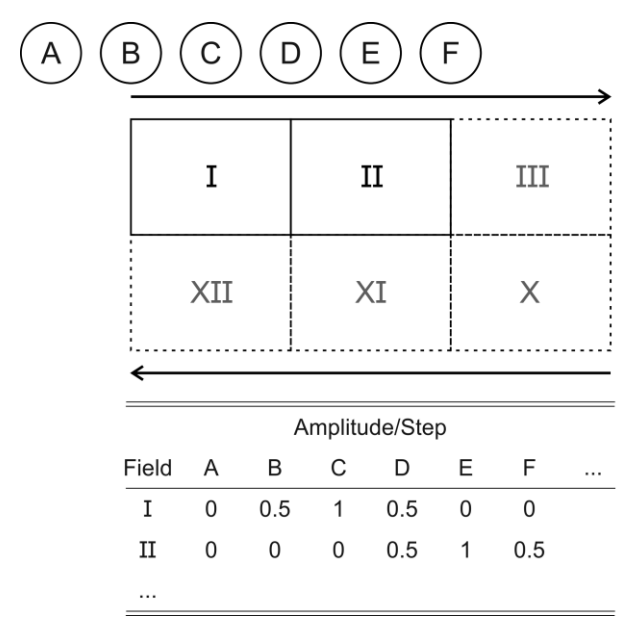


Figure 22. Heat flux amplitudes on the individual fields of the coating area as a function of time.

The in this way simulated temperature trends are compared to the measured ones in Figure 23, with the corresponding heat flows and fluxes utilized in the different steps of preheating and coating additionally noted in the charts. In case of the smaller Mock-ups (Figure 23 a and b), the temperatures decrease at the beginning of the coating step, in which a smaller heat flux is used than during preheating. This implies that in the simulation heat accumulated during preheating in the area of the cooling channels, possibly due to the lesser amount of material for heat transfer. This heat accumulation can then dissipate under the lower heat flux during coating and a new equilibrium of heat input and transfer develops. In regard to the larger Mock-up (Figure 23 c), an interruption and change of the temperature slopes exist during preheating, because the Mock-up was first preheated at a lower power level, to observe the behaviour of the setup, and then the power was increased to normal levels.

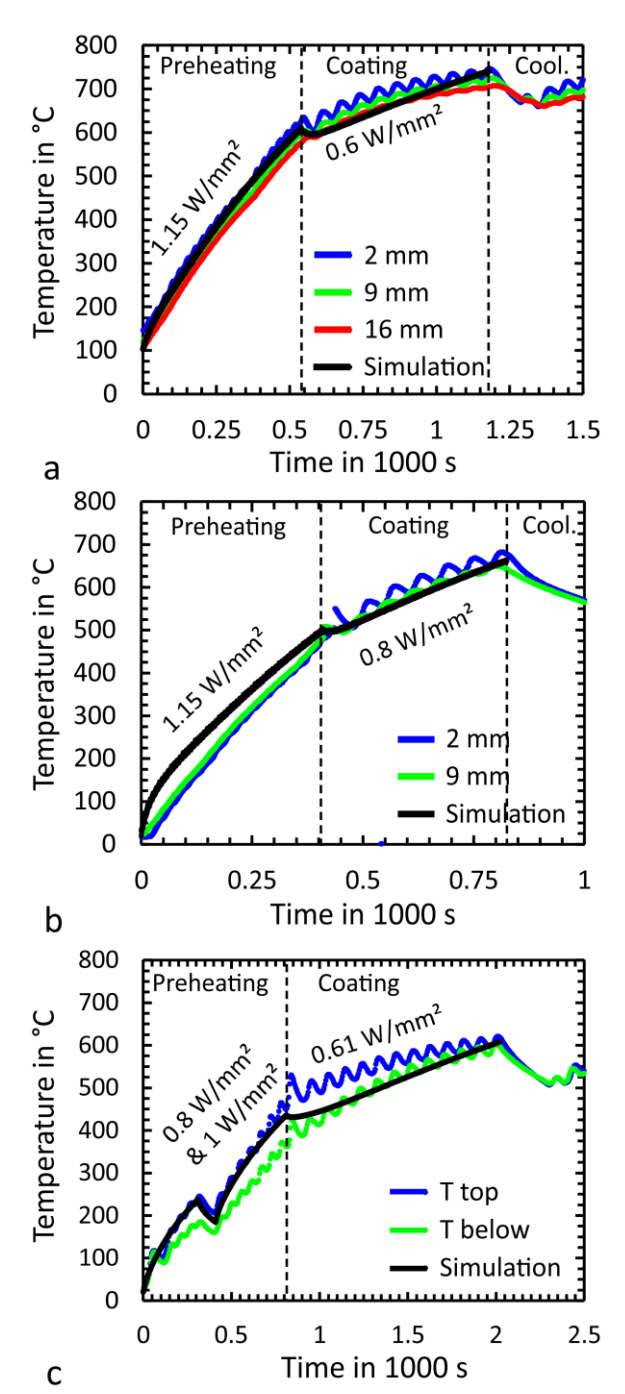


Figure 23. Comparison of the measured and simulated temperature trends for (a) the first small test Mock-up, (b) the second small test Mock-up, coated with a lower maximum temperature, and (c) the larger Mock-up.

Based on these simulations the temperatures at the coating area corners can also be approximated from the simulations data. The corners are of special interest, because there the temperatures could

be minimal and the layers susceptible for delamination, due to the distance to the coating area center and geometry, respectively.

In case of the first smaller Mock-up (Figure 24 a) the temperatures equal after preheating 605 °C at the center and 460 °C at the corners, while for the second Mock-up (Figure 24 b) the corresponding temperatures are 495 °C and 350 °C. In case of the larger Mock-up (Figure 24 c), however, the temperatures amount after preheating only to about 440 °C at the center and 265 °C at the corners, which are apparently too low for the development of a sufficient layer adhesion. Therefore, the preheating temperatures like in the successfully coated second smaller Mock-up (≥ 500 °C) are assumed as minimal preheating temperature. However, these temperatures are also not achieved even if a heat flux of 1 W/mm² is used from the start for the same preheating duration (Figure 24 d). Hence, longer preheating is necessary, which will, though, intensify the temperature difference between the center and the corners due to the different temperature increases. To avoid overheating in the center by heat accumulation and achieve a heating of the coating area as homogeneously as possible the preheating could be suspended for e.g. five minutes. This allows the heat accumulation to dissipate, so that the temperature difference is reduced from nearly 200 °C to about 90 °C. During an additional preheating, with the same heat flux, temperatures like for the test Mock-ups can be achieved (Figure 24 d). Proceeding from these preheating with the coating, also similar temperatures are generated after the duration of 1200 s correspondingly to the first and second small Mock-up (Figure 25).

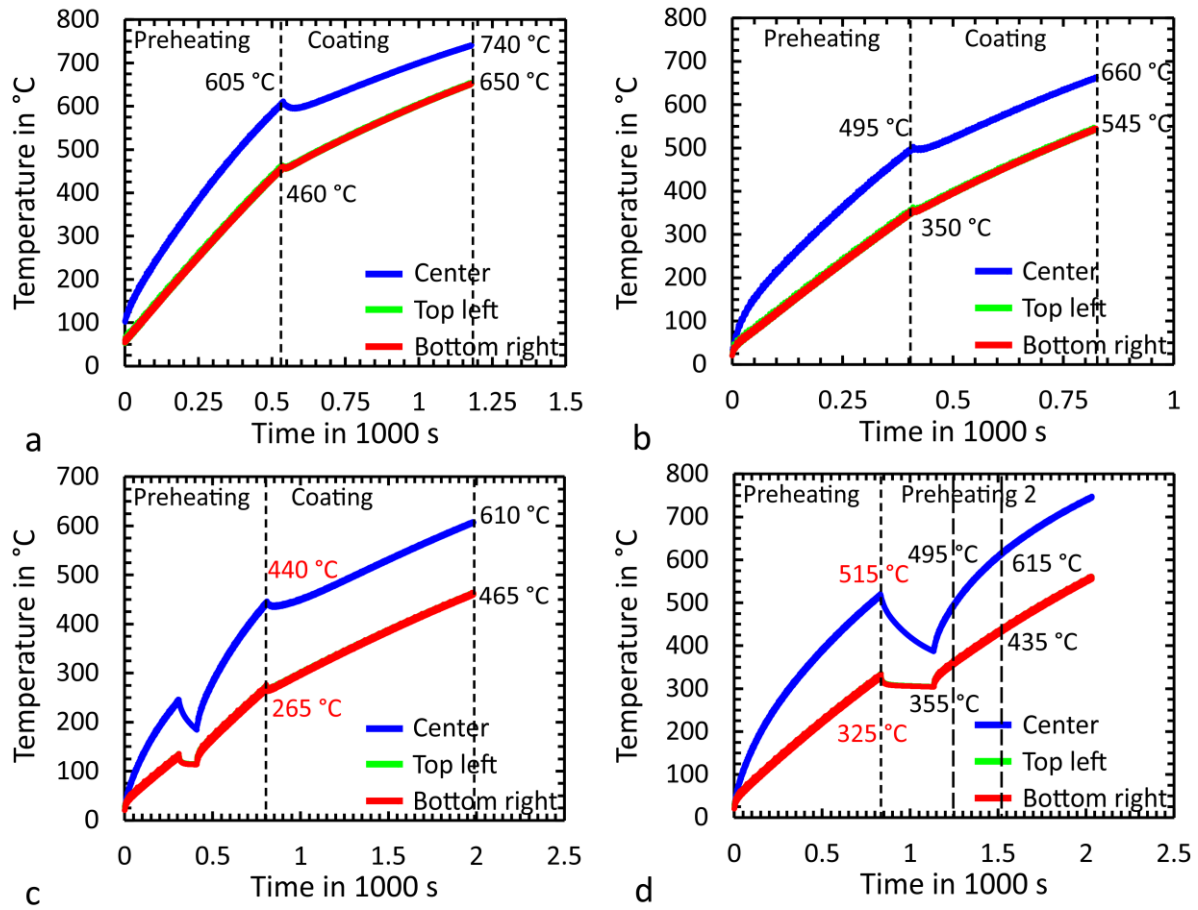


Figure 24. Simulated temperature trends for the center and the corners of the coating area of (a) the first small Mock-up, (b) the second small Mock-up, coated with a lower maximum temperature, (c) the larger Mock-up and (d) the larger Mock-up with additional preheating.

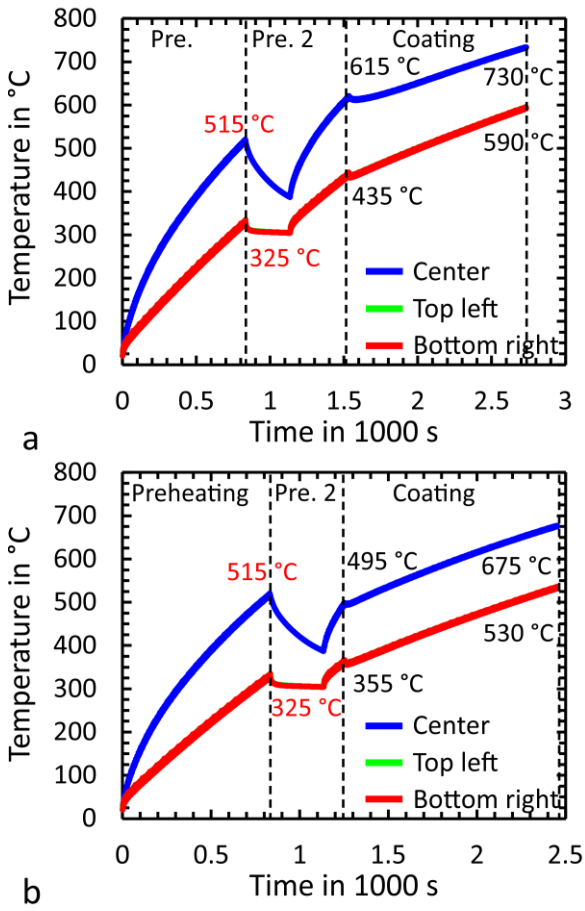


Figure 25. Simulated temperature trends for the center and the corners of the coating area of the larger Mock-up starting from an initial coating temperature similar to (a) the first small Mock-up and (b) the second small Mock-up, coated with a lower maximum temperature.

In view of widening the FG-coating to the whole surface, the preheating can also be performed on a larger area. This is reproduced in the thermal analysis by extending the coating area on the model (Figure 21) to 270×200 mm² and dividing it into 24 fields of 45×50 mm². Due to the larger area the heat flux of 1 W/mm² can be applied to, surface temperatures, like for the second and first smaller Mock-ups, are already achieved after 835 and 950 s, respectively (Figure 26). Therefore, an additional preheating is not required. A short break of about 180 s allows the temperature difference between the center and the corners to dissipate from around 130 to about 105 °C. Continuing from this point with the coating, the surface reaches after a duration of 1200 s temperatures of 755 and 645 °C or 730 and 620 °C, respectively. The higher temperatures of the first trend would be

advantageous for developing good layer adhesion [2], though, but the latter trend was chosen for anew coating of the larger Mock-up, due to the limitations of the substrate tempering temperature and the limited heat management of the utilized VPS-facility.

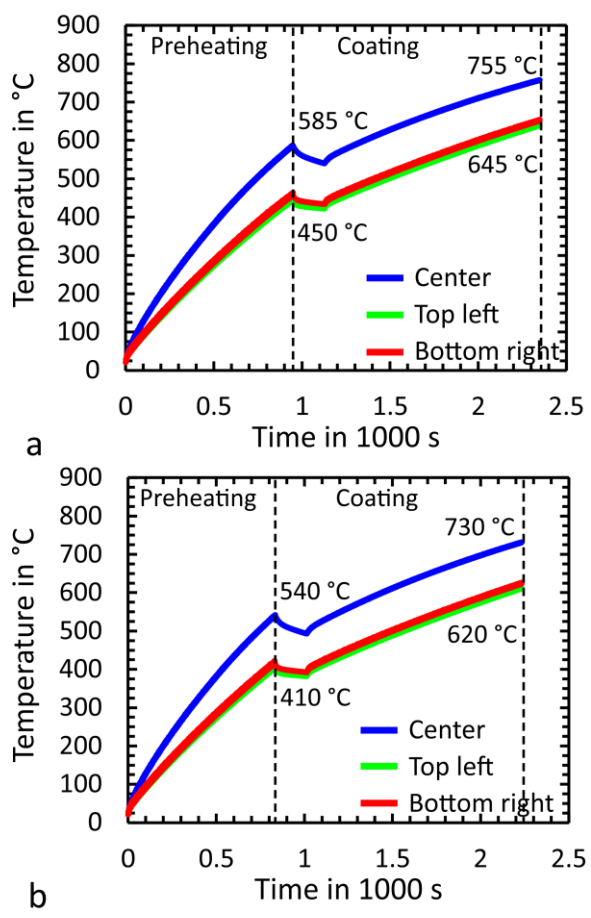


Figure 26. Simulated temperature trends for the center and the corners of the enlarged coating area of the larger Mock-up starting from an initial coating temperature similar to (a) the first small Mock-up and (b) the second small Mock-up, coated with a lower maximum temperature.

4.3. Coating using optimised coating process

Based on the studies above, the anew coating was successfully deposited on the Mock-up with a larger FG-coating area, gently inclining slopes and modified preheating. Neither external nor internal adhesion defects were detected and particularly in the central part, the cooling channels with the cooling ribs are clearly depicted by the ultrasonic testing (Figure 27).

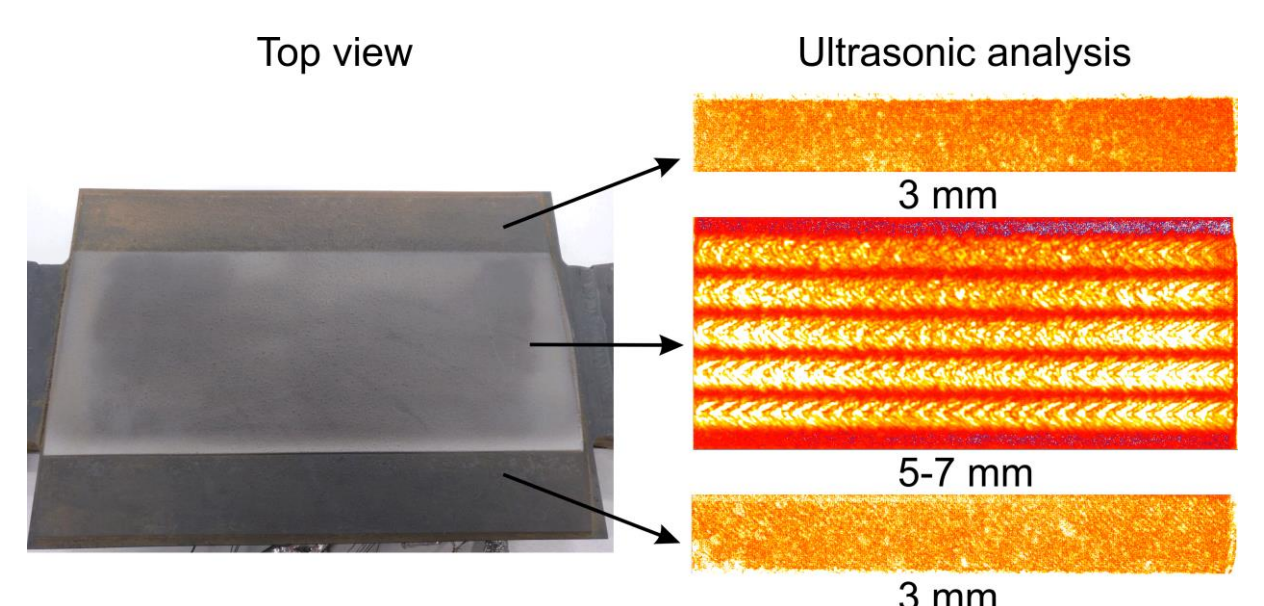


Figure 27. Top view on the larger Mock-up with second coating after the ultrasonic testing and the results of the latter with the specific analysis depths.

Figure 28 presents the measured temperature trends during the anew coating at the three locations specified in Figure 13. The figure emphasises the required effort for the production, as the process has to be interrupted and restarted several times, so that the VPS-facility itself is able to cool down. In contrast to the performed simulations, however, the temperature differences are clearly smaller than 100 °C and often in the range of only about 60 °C, while the temperatures at the perpendicular position is often higher than at the other two locations. The lower temperature discrepancies indicate that the materials thermal conductivity is actually larger than the assumed values (Table 6), which were extrapolated from data that was experimentally determined only up to about 600 °C [12]. At this point it shall be remarked on a side note that equation (9) [12] already provides larger thermal conductivity values than equation (10) [12]. A higher thermal conductivity correlates, first of all, to the determined substrate hardness profiles of the smaller Mock-ups (Figure 10), from which followed that a local heat accumulation above the cooling channels did not occur. Secondly, the apparently higher thermal conductivity is also corroborated by the wavelike temperature trends, e.g. Figure 23, indicating that the heat from the spraying plasma plume dissipates faster than calculated by the FE-simulations. The wavelike temperature trends imply

further that the heat flux of the sprayed powder was higher than the fitted values. In regard to the comparatively higher temperature at the perpendicular position, the respective measurements could have been influenced by the massive side parts (Figure 13), which emit their stored heat.

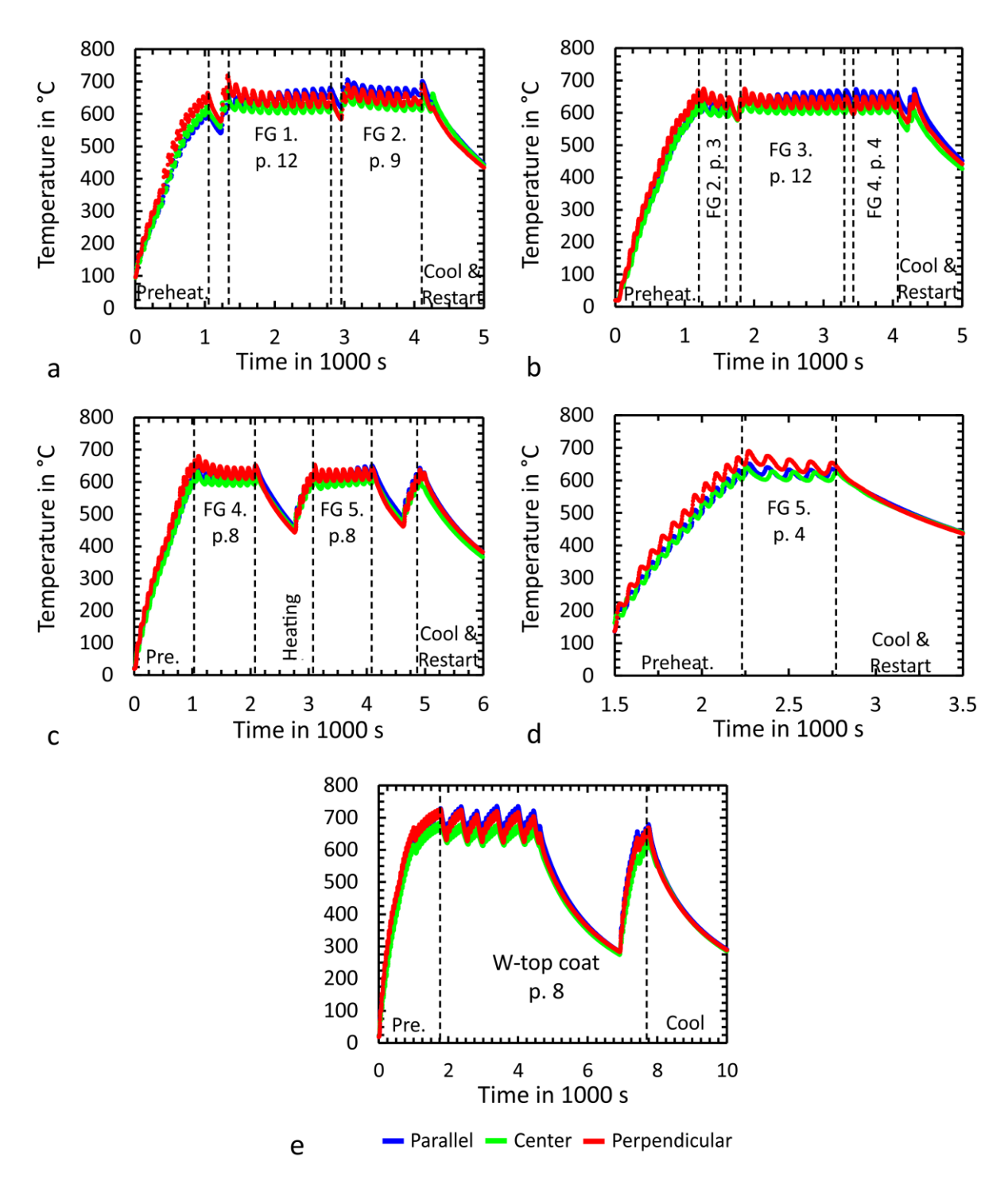


Figure 28. Temperatures in the larger Mock-up, at the three locations indicated by Figure 13, during preheating, coating and cooling, with the respective number of passes (p.) of the spraying system for depositing (a-d) the FG-layers and (e) the W-top coat.

After the successful coating the Mock-up was controlled in regard to pressure vessel standards and subjected to required repair welding, which was performed, based on the gained experience from the previous Mock-up, only locally. Subsequently, the Mock-up was heat treated in a vacuum furnace for 2 h at 740 °C with furnace cooling to room temperature and no delamination of the coating occurred. Finally, the Mock-up was qualified by a conducted pressure test.

In view of previous works to optimize the coating [7], the in this work presented experiments show that a significant cooling of the substrate is not a feasible option. It is theoretically attractive, due to lower temperatures and thus less thermal stress, but sufficient bonding is not achieved on a substrate colder than about 500 °C. For future larger components active cooling may, nevertheless, still be an option, to remove at coating temperature the heat from the plasma plume faster and thus improve the process time and reduce the thermal load on the facility.

5. Summary and Outlook

In this paper following work on the development of FG W/EUROFER-coatings for future First Wall components was conducted and promising results gained:

- 1. An overview of thermomechanical material properties was given.
- 2. First Wall Mock-ups were manufactured and successfully coated on areas of 270×65 mm².
- 3. One coated Mock-up was successfully tested under fusion relevant heat loads and Helium flows in HELOKA and the durability of the coating system confirmed.
- 4. Another, larger Mock-up was manufactured and successfully coated with the functionally graded layer system on an area of 270×200 mm² and the tungsten-top coat on an area of 270×115 mm², after a process optimization supported by FE-simulations.

For future, even larger Mock-ups or full scale components, coating on laboratory scale is no longer possible. Therefore, first development tests of coating on industry scale will be carried out.

In parallel, further durability tests of the coating systems under fusion relevant conditions need to be conducted.

Acknowledgment

This work has been carried out within the framework of the EUROfusion Consortium and has received funding from the Euratom research and training programme 2014-2018 and 2019-2020 under grant agreement No 633053. The views and opinions expressed herein do not necessarily reflect those of the European Commission. The authors wish to thank the colleagues from the Institute for Applied Materials – Applied Material Physics for the chemical analysis of the steel powder and the thermal diffusivity measurements.

References

- [1] D.D. Qu, W.W. Basuki, J. Aktaa, Numerical assessment of functionally graded tungsten/EUROFER coating system for First Wall applications, Fusion Eng. Des. 98-99 (2015) 1389–1393. https://doi.org/10.1016/j.fusengdes.2015.06.120.
- [2] R. Vaßen, K.-H. Rauwald, O. Guillon, J. Aktaa, T. Weber, H.C. Back, D. Qu, J. Gibmeier, Vacuum plasma spraying of functionally graded tungsten/EUROFER97 coatings for fusion applications, Fusion Eng. Des. 133 (2018) 148–156. https://doi.org/10.1016/j.fusengdes.2018.06.006.
- [3] D. Qu, Development of functionally graded tungsten/EUROFER coating systems. PhD Thesis, Karlsruhe, 2016.
- [4] J. Aktaa, D.D. Qu, Spraying 2 mm thick coating system and optimising the spray parameters. EUROfusion IDM EFDA_D_2MLW4C, 2016.
- [5] D.D. Qu, W.W. Basuki, J. Gibmeier, R. Vaßen, J. Aktaa, Development of functionally graded tungsten/EUROFER coating system for First Wall application, Fusion Sci. Technol. 68 (3) (2015) 578–581. https://doi.org/10.13182/FST15-113.

- [6] R. Lindau, et al., Present development status of EUROFER and ODS-EUROFER for application in blanket concepts, Fusion Eng. Des. 75-79 (2005) 989–996. https://doi.org/10.1016/j.fusengdes.2005.06.186.
- [7] T. Emmerich, D.D. Qu, R. Vaßen, J. Aktaa, Development of W-coating with functionally graded W/EUROFER-layers for protection of First-Wall materials, Fusion Eng. Des. 128 (2018) 58–67. https://doi.org/10.1016/j.fusengdes.2018.01.047.
- [8] T. Weber, J. Aktaa, Numerical assessment of functionally graded tungsten/steel joints for divertor applications, Fusion Eng. Des. 86 (2-3) (2011) 220–226. https://doi.org/10.1016/j.fusengdes.2010.12.084.
- [9] T. Weber, M. Stüber, S. Ulrich, R. Vaßen, W.W. Basuki, J. Lohmiller, W. Sittel, J. Aktaa, Functionally graded vacuum plasma sprayed and magnetron sputtered tungsten/EUROFER97 interlayers for joints in helium-cooled divertor components, J. Nucl. Mater. 436 (1-3) (2013) 29–39. https://doi.org/10.1016/j.jnucmat.2013.01.286.
- [10] T. Emmerich, R. Vaßen, J. Aktaa, Thermal fatigue tests on functionally graded W/EUROFER-layer systems in a newly constructed testing apparatus, ISFNT-14 Budapest, 2019.
- [11] T. Nagasaka, Thermophysical properties and microstructure of plasma-sprayed tungsten coating on low activation materials, Fusion Sci. Technol. 56 (2) (2009) 1053–1057. https://doi.org/10.13182/FST56-1053.
- [12] K. Mergia, N. Boukos, Structural, thermal, electrical and magnetic properties of Eurofer 97 steel, J. Nucl. Mater. 373 (1-3) (2008) 1–8. https://doi.org/10.1016/j.jnucmat.2007.03.267.
- [13] VdTÜV, Warmfester Stahl X10CrWMoVNb9-2; Werkstoff-Nr. 1.4901, Verband der TÜV e.V., Köln, 2009.
- [14] F. Arbeiter, C. Bachmann, Y. Chen, M. Ilić, F. Schwab, B. Sieglin, R. Wenninger, Thermal-hydraulics of helium cooled First Wall channels and scoping investigations on performance

- improvement by application of ribs and mixing devices, Fusion Eng. Des. 109-111 (2016) 1123–1129. https://doi.org/10.1016/j.fusengdes.2016.01.008.
- [15] V. Kuznetsov, Cr-Fe-W, in: W. Martienssen, G. Effenberg, S. Ilyenko (Eds.), Refractory metal systems, Springer Berlin Heidelberg, Berlin, Heidelberg, 2010.
- [16] H. Neuberger, J. Rey, A. von der Weth, F. Hernandez, T. Martin, M. Zmitko, A. Felde, R. Niewöhner, F. Krüger, Overview on ITER and DEMO blanket fabrication activities of the KIT INR and related frameworks, Fusion Engineering and Design 96-97 (2015) 315–318. https://doi.org/10.1016/j.fusengdes.2015.06.174.
- [17] Dassault Systèmes Simulia Corp., ABAQUS, 2016.